Heavy Flavor Production in ATLAS: Charmonium production in p-p at 13 TeV and in Pb-Pb collisions. Associated charmonium and Vector boson production

Brad Abbott

University of Oklahoma

On behalf of the ATLAS Collaboration

Outline

Heavy Ion Results

Charmonium Production in Pb-Pb Eur. Phys. J. C78 (2018) 762

Quarkonium production in pp and pPb Eur. Phys. J. C 78 (2018) 171

J/ψ elliptic flow in Pb-Pb Eur. Phys. J. C 78 (2018) 784

Heavy Flavor Production

J/ψ and ψ(2S) production cross sections at high p_T at 13 TeV ATLAS-CONF-2019-047

J/ψ production in associated with a W boson at 8 TeV arXiv:hep-ex 1909.13626

Charmonium Production in Pb-Pb

Eur. Phys. J. C78 (2018) 762

Charmonium Production in Pb-Pb

Eur. Phys. J. C78 (2018) 762

Modification of prompt J/ψ production is not expected to be similar to non-prompt J/ψ production since different mechanisms contribute to the final states

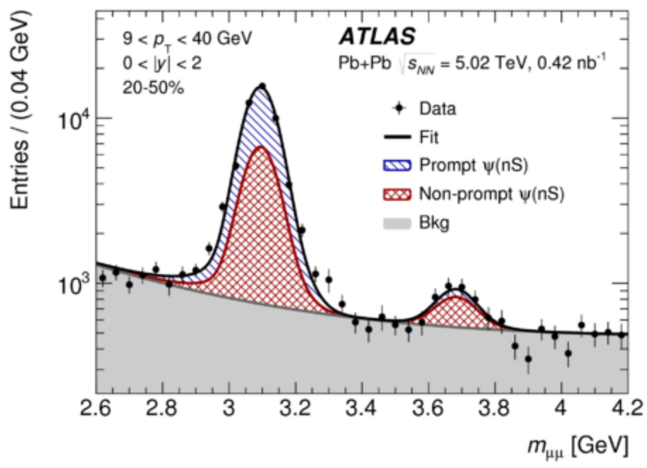

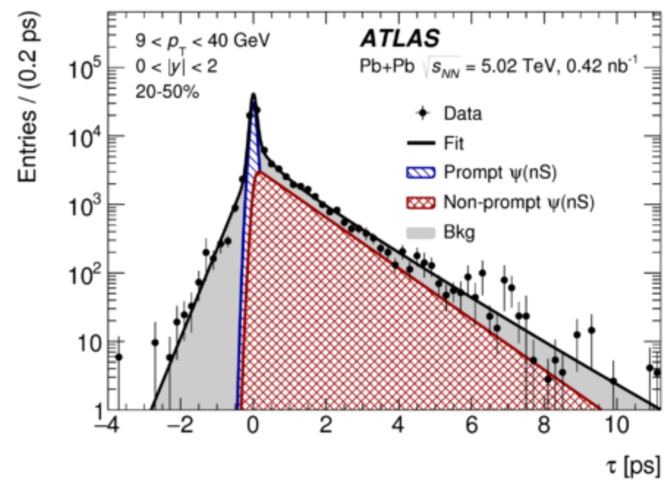

$$\tau = \frac{L_{xy} m_{\mu\mu}}{p_T^{\mu\mu}}$$

Use simultaneous mass/lifetime fits to extract prompt/non-prompt component

Extract yields as a function of p_T, y and centrality

Centrality: $\sum E_T^{FCal}$ Measures degree of geometrical overlap of two colliding nuclei in the plane perpendicular to the beam.

Each event corrected for acceptance, reconstruction efficiency and trigger efficiency

Nuclear Modification Factor R_{AA}

$$R_{AA} = \frac{Per\ Event\ Yield}{Mean\ Nuclear\ Thickness * Cross\ Section}$$

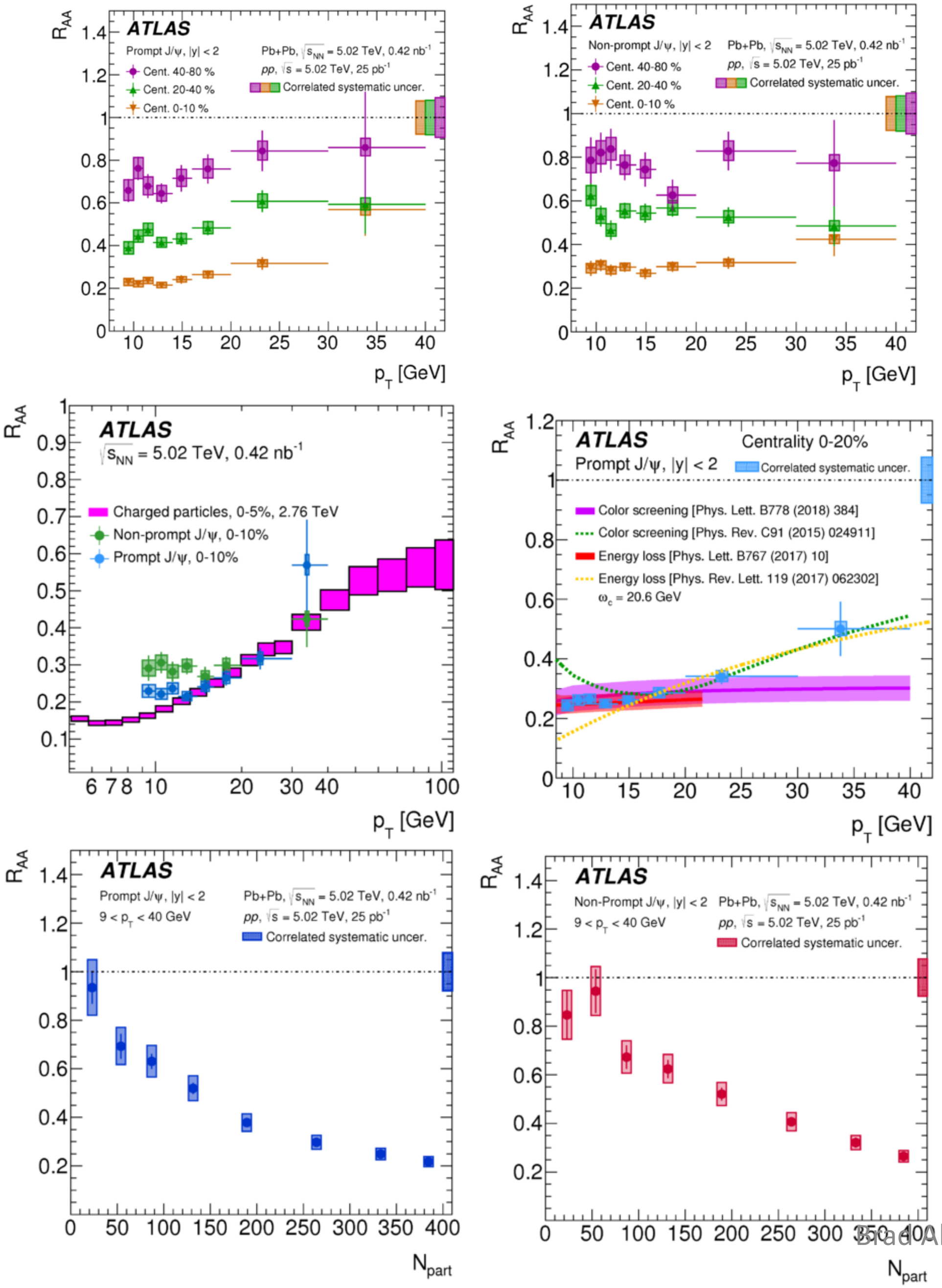

Production of J/ψ strongly suppressed in central Pb-Pb collisions

Non-prompt consistent with flat

For p_T>12 GeV small increase in R_{AA}

Consistent with color screening and parton-energy loss models

Suppression sign that the hot dense medium has a strong influence on particle production processes

Both prompt and non-prompt have similar behavior. Not expected since non-prompt dominated by b-decays that extend outside medium while prompt production happens primarily within medium

Double ratio: $(\psi(2s)/J/\psi)$Pb+Pb $/(\psi(2S)/J/\psi)$pp

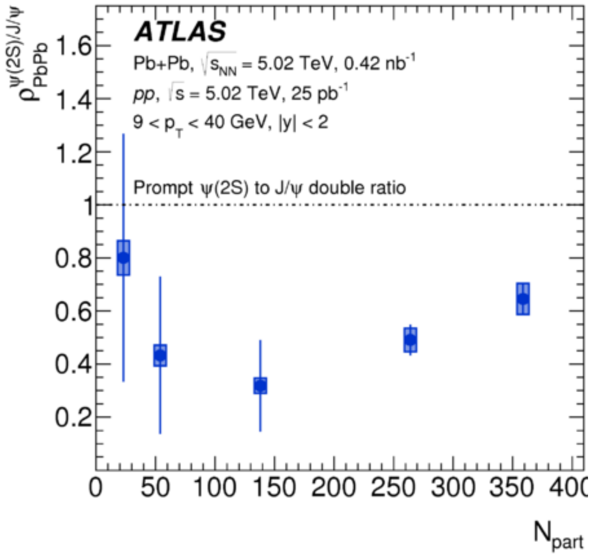

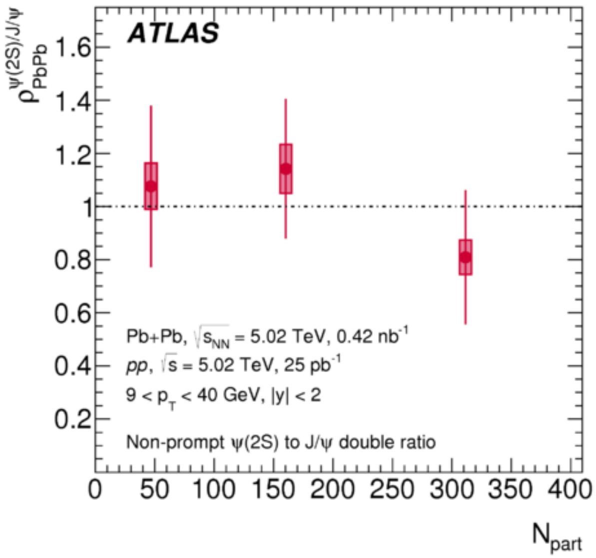

If non-prompt J/ψ and $\psi(2s)$ originate from b-quarks losing energy in medium and hadronizing outside medium, ratio should be unity

Prompt J/ψ and $\psi(2s)$ should traverse medium

Non-prompt consistent with unity suggesting both mesons originate from b-quarks

Consistent with interpretation that the tighter bound J/ψ survives in the hot and dense medium with higher probability than the more loosely bound $\psi(2S)$.

Quarkonium production in pp and pPb

Eur. Phys. J. C 78 (2018) 171

Quarkonium production in pp and pPb

Eur. Phys. J. C 78 (2018) 171

Study of suppression
of charmonium
in pp and p-Pb

Simultaneous mass/lifetime
fit in bins of P_T , rapidity
and centrality for charmonium

Mass fits in bins of P_T,
rapidity and centrality
for bottomonium

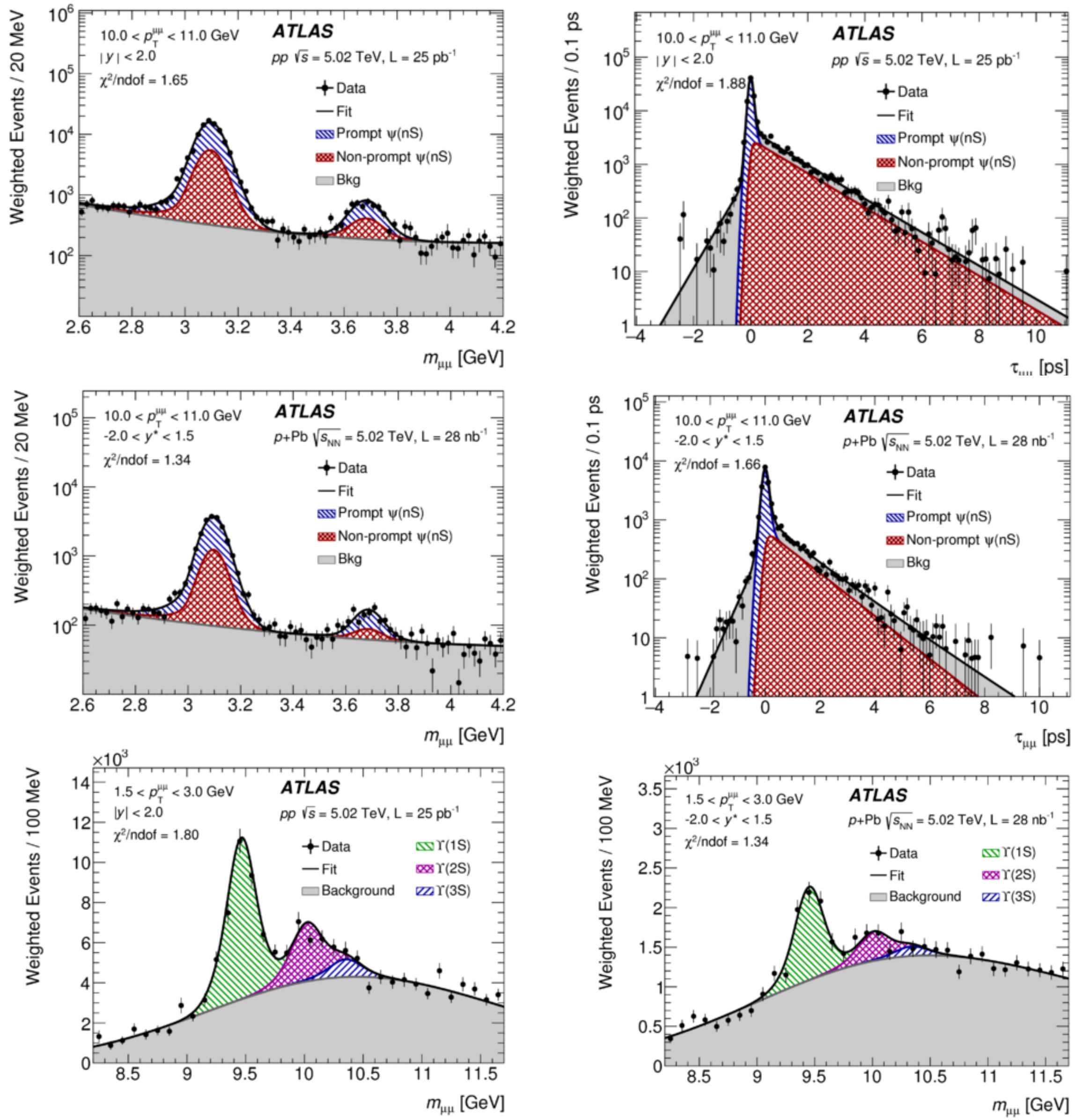

Events weighted for efficiency and acceptance

Differential pp results

$$\frac{d^2\sigma_{O(nS)}}{dp_T dy^*} \times B(O(nS) \to \mu^+\mu^-) = \frac{N_{O(nS)}}{\Delta p_T \times \Delta y \times L}$$

In pp collisions:
Prompt: Charmonium good agreement observed between data and NRQCD

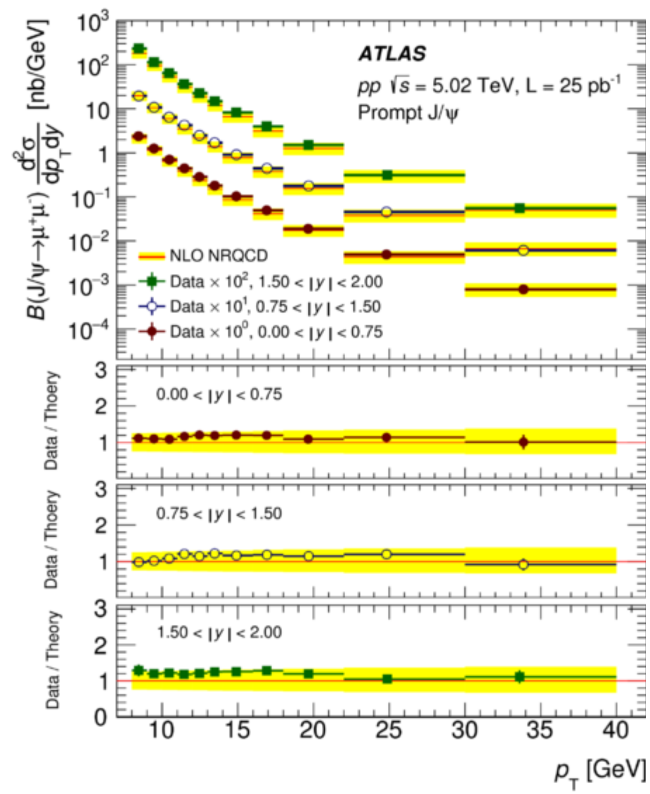

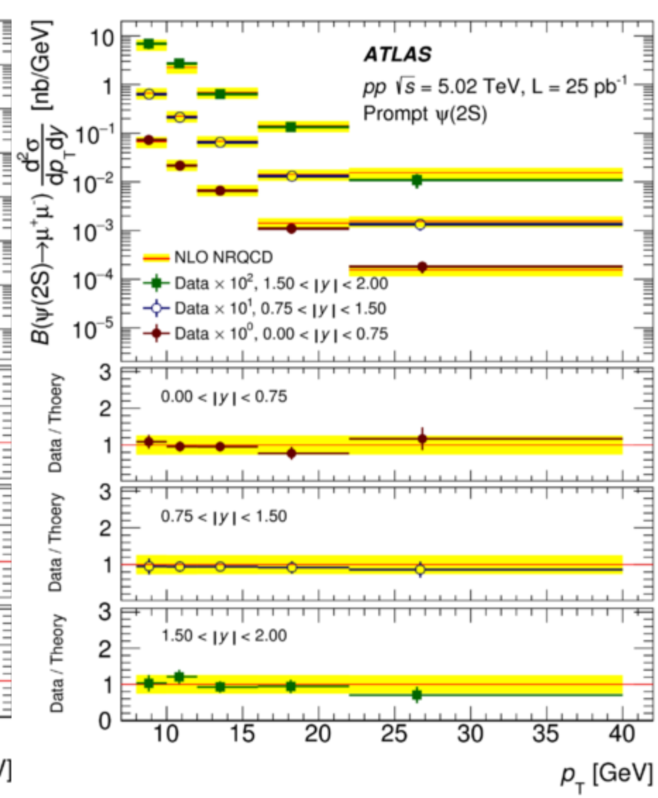

y*: proton-nucleon center of mass rapidity

NRQCD: PRL **106** (2011) 042002, JHEP **05** (2015) 103

Differential pp results

$$\frac{d^2\sigma_{O(nS)}}{dp_T dy^*} \times B(O(nS) \rightarrow \mu^+\mu^-) = \frac{N_{O(nS)}}{\Delta p_T \times \Delta y \times L}$$

In pp collisions:
Non-prompt: Charmonium good agreement observed between data and FONLL

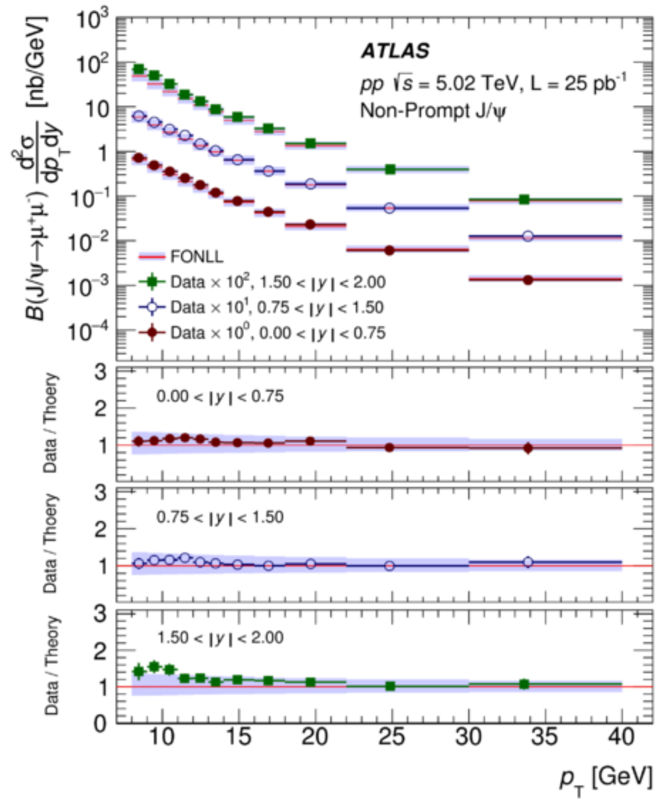

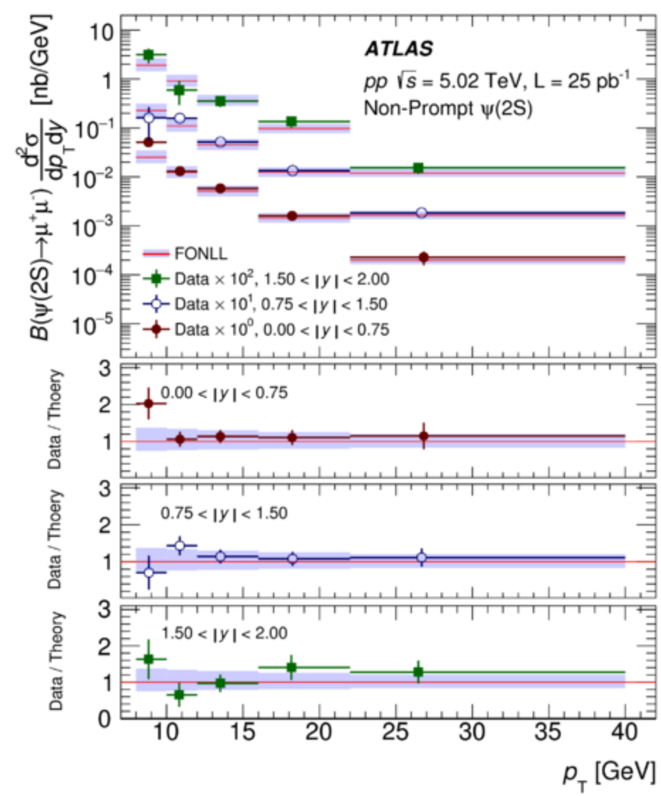

FONLL: JHEP **10** (2012) 137

Differential pp results

$$\frac{d^2\sigma_{O(nS)}}{dp_T dy^*} \times B(O(nS) \rightarrow \mu^+\mu^-) = \frac{N_{O(nS)}}{\Delta p_T \times \Delta y \times L}$$

In pp collisions:
Bottomonium
agreement observed
between data and NRQCD
for p_T>15 GeV

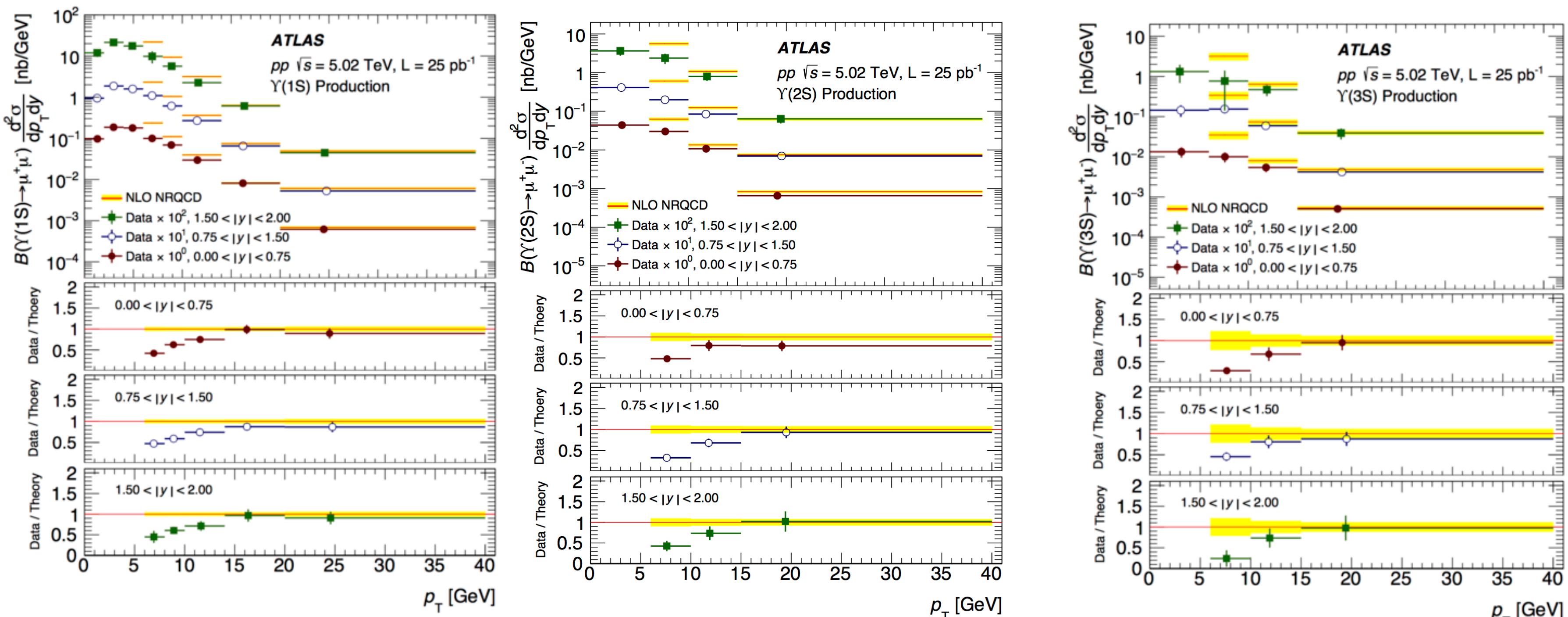

NRQCD: Phys. Rev. D **94** (2016) 014028

Nuclear modification factors

$$R_{pPb} = \frac{1}{208}\frac{\sigma^{O(nS)}_{p+pb}}{\sigma^{O(nS)}_{pp}}$$

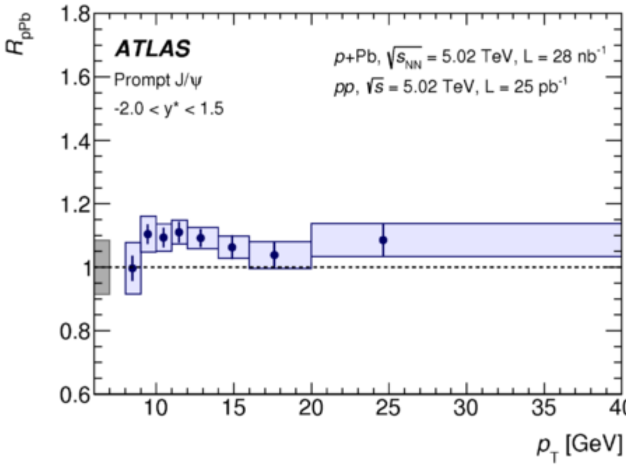

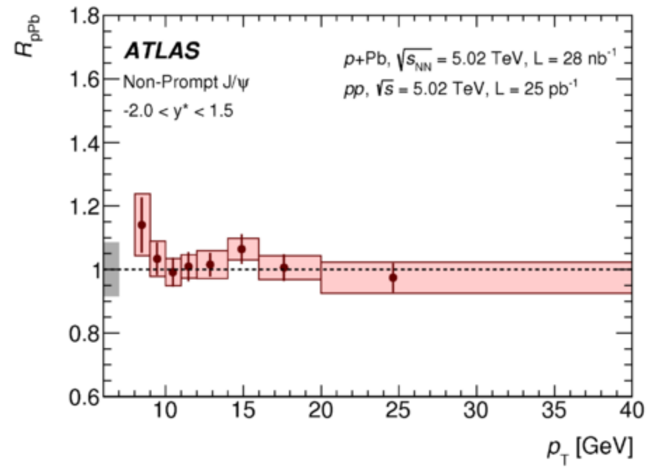

Prompt and non-prompt J/ψ consistent with unity across p_T range 8-40 GeV

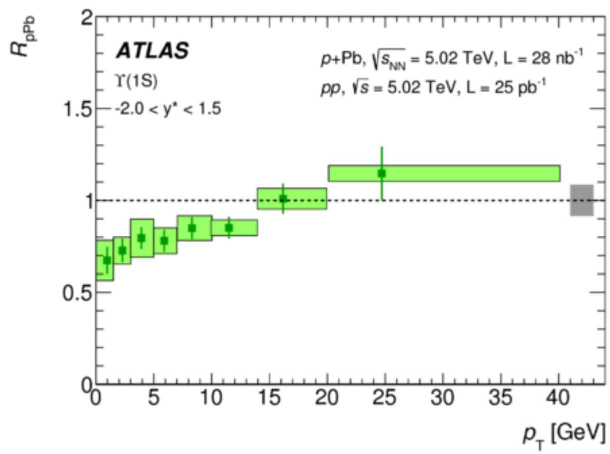

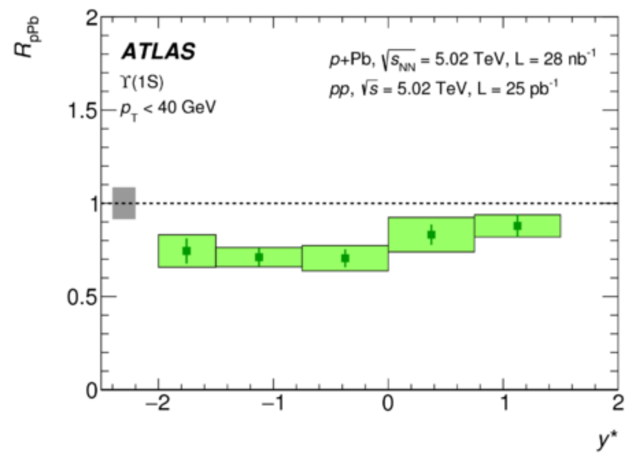

ϒ(1s) shows significant discrepancy with unity at low p_T

Low p_T ϒ(1S) can probe smaller Bjorken-x region compared to J/ψ measured in $8<p_T<40$ GeV

Observed suppression of ϒ(1S) may come from the reduction of hard-scattering cross sections due to strong nPDF shadowing at smaller Bjorken-x

Double production ratio

$$\rho_{pPb}^{O(nS)/O(1S)} = \frac{R_{pPb}(O(nS))}{R_{pPb}(O(1S))} = \frac{\sigma_{p+Pb}^{O(nS)}}{\sigma_{p+Pb}^{O(1S)}} / \frac{\sigma_{pp}^{O(nS)}}{\sigma_{pp}^{O(1S)}}$$

Suppression of Υ(3S) and O(2S) states wrt O(1S) between 1-2 sigma

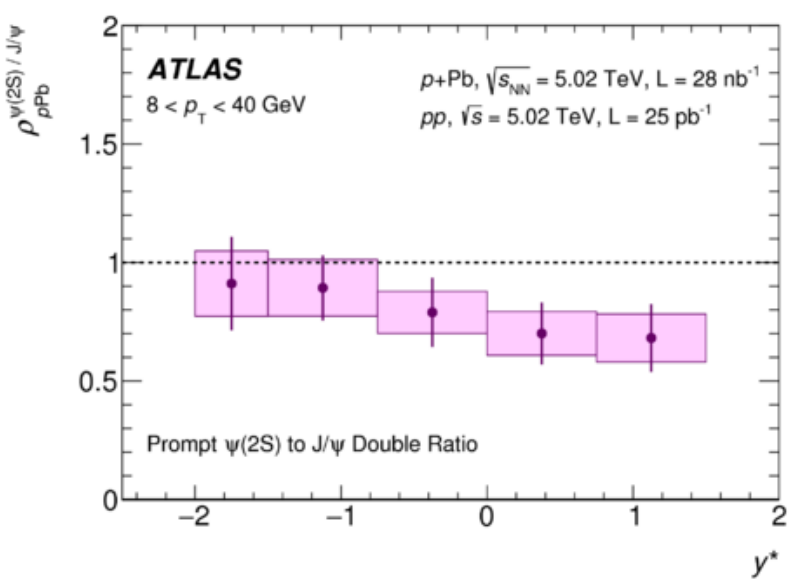

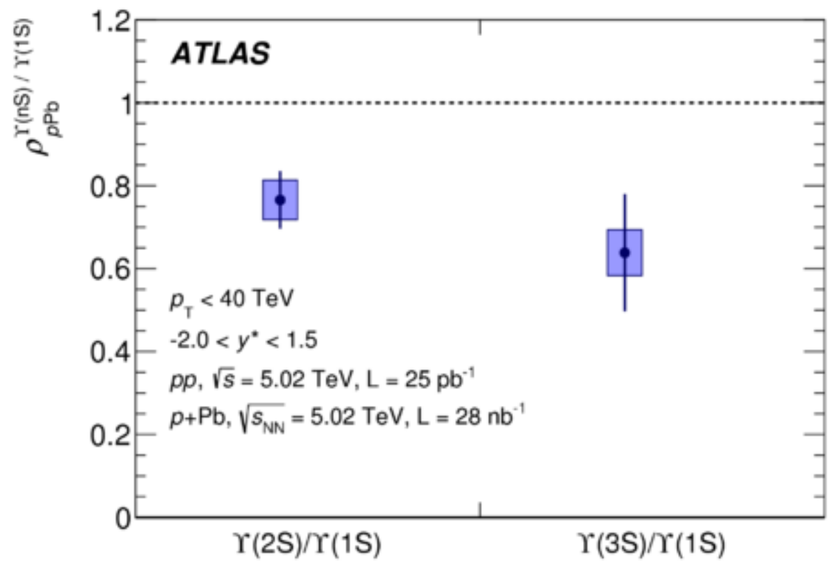

Double production ratio

$$\rho_{pPb}^{O(nS)/O(1S)} = \frac{R_{pPb}(O(nS))}{R_{pPb}(O(1S))} = \frac{\sigma_{p+Pb}^{O(nS)}}{\sigma_{p+Pb}^{O(1S)}} / \frac{\sigma_{pp}^{O(nS)}}{\sigma_{pp}^{O(1S)}}$$

Decreasing trends from peripheral to central are at the significance level of 1 sigma

A stronger cold nuclear matter effect is observed in excited quarkonium states compared to that in ground states.

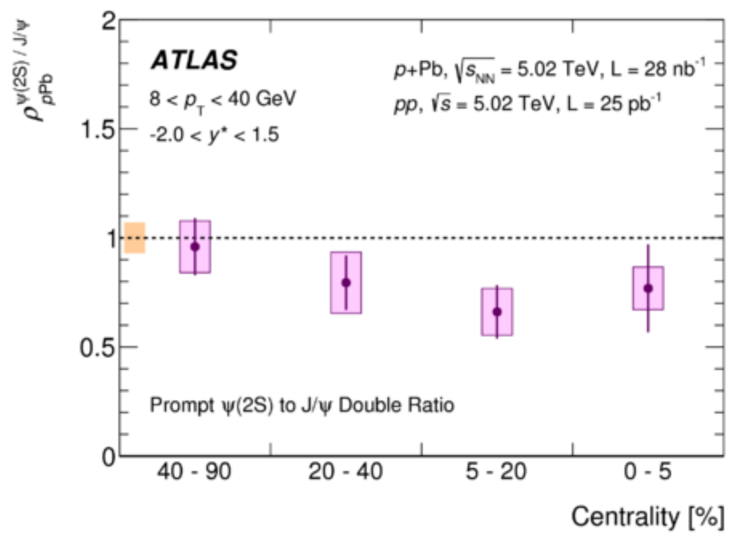

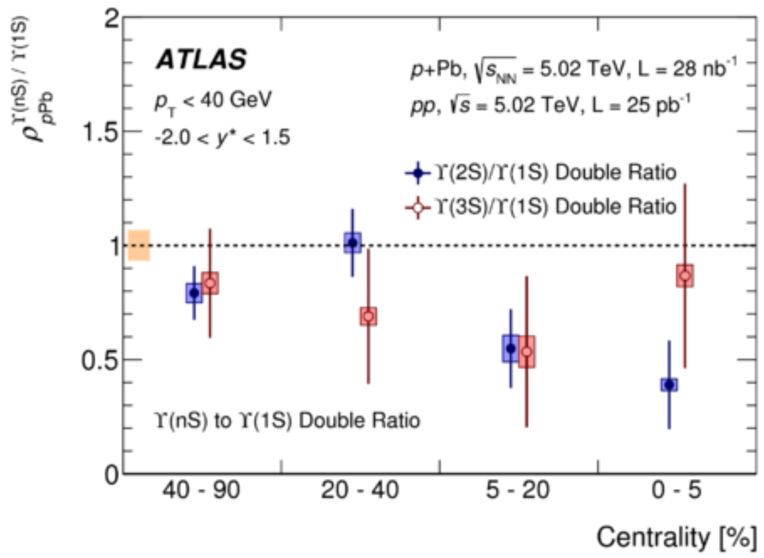

J/ψ elliptic flow in Pb-Pb

Eur. Phys. J. C 78 (2018) 784

J/ψ elliptic flow in Pb-Pb

Eur. Phys. J. C 78 (2018) 784

Compare prompt vs non prompt J/ψ probes flavor dependence of the medium.

Study azimuthal distribution of particles characterized by $\frac{dN}{d\phi} \sim 1 + \sum_{n=1}^{\infty} 2v_n \cos[n(\phi - \psi_n)]$

v_2: Elliptic flow

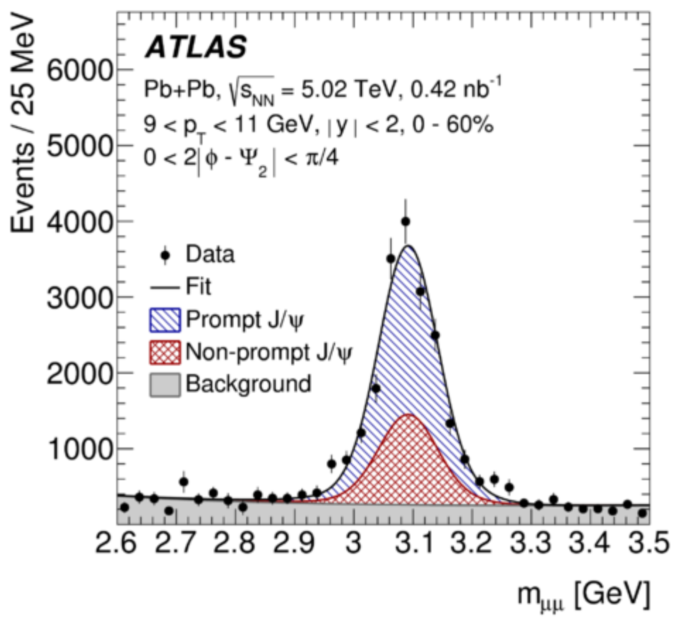

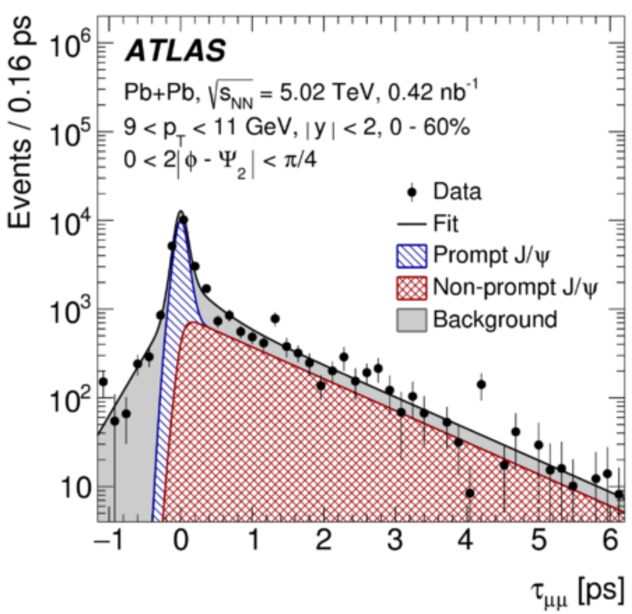

Events weighted for efficiency and acceptance

Decreasing v_2 with increasing p_T for prompt J/ψ

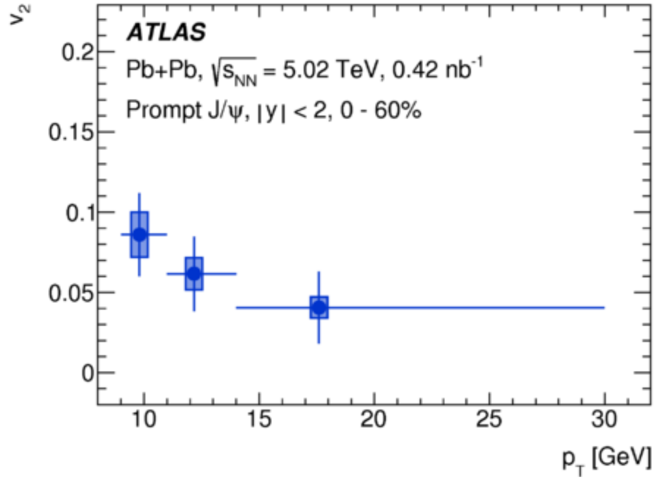

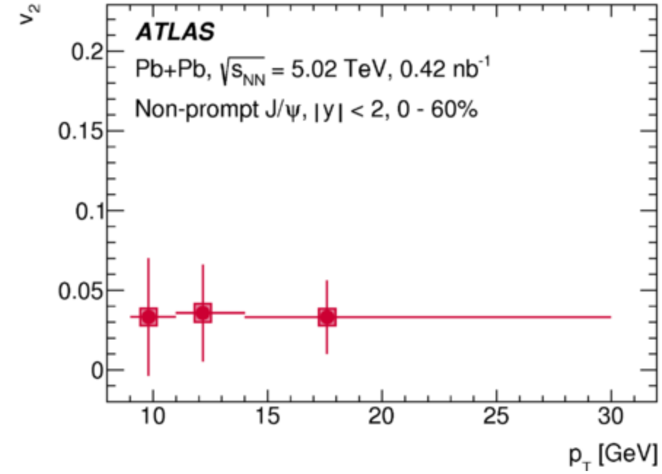

No significant rapidity or centrality (not shown dependence seen

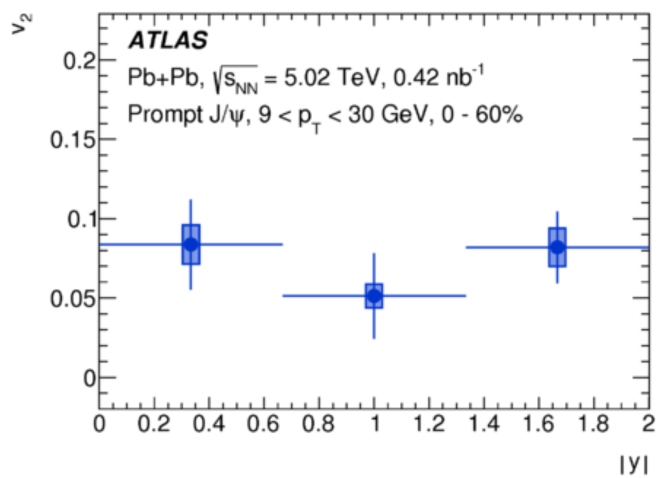

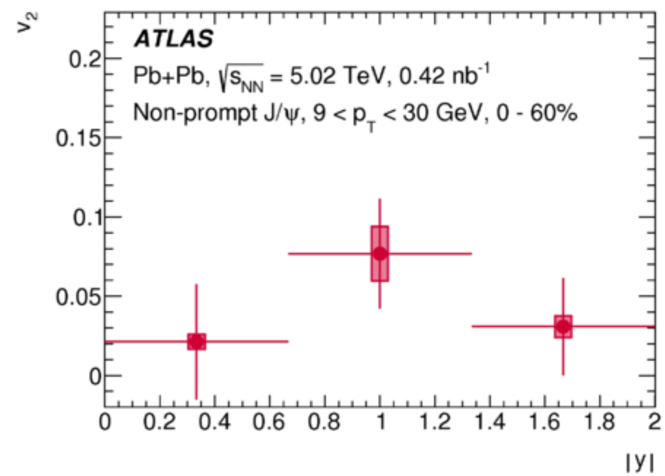

At high p_T, similar v_2 for prompt and non-prompt suggesting similar suppression mechanism at high p_T

Measurement of the production cross-section of J/ψ and ψ(2S) mesons at high transverse momentum at 13 TeV

https://atlas.web.cern.ch/Atlas/GROUPS/PHYSICS/CONFNOTES/ATLAS-CONF-2019-047

Provides insight into QCD near boundary of perturbative and non-perturbative regimes

Previous measurements of cross sections used dimuon triggers with low thresholds

Dimuon triggers could not reach beyond p_T of ~ 100 GeV

Measuring high-p_T production of quarkonium states important because high p_T behavior may help discriminate various theoretical models

Previous measurements reached J/ψ p_T of 150 GeV
Phys. Lett. B **780** (2018) 251

Single muon triggers and full run-2 dataset allows measurement at high p_T (60-360 GeV) significantly expanding range

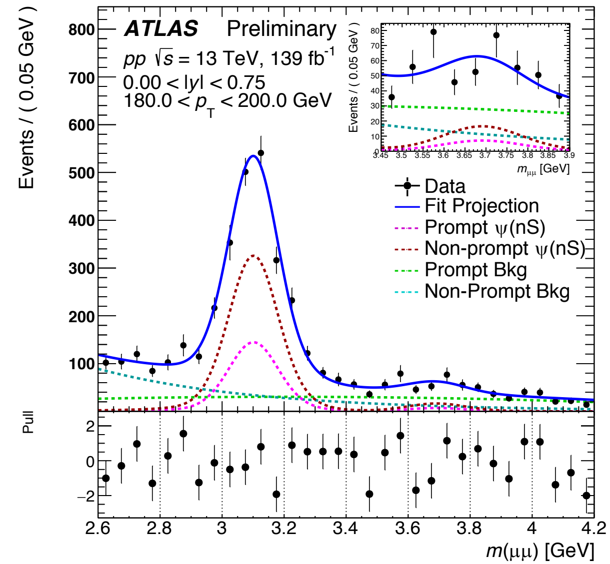

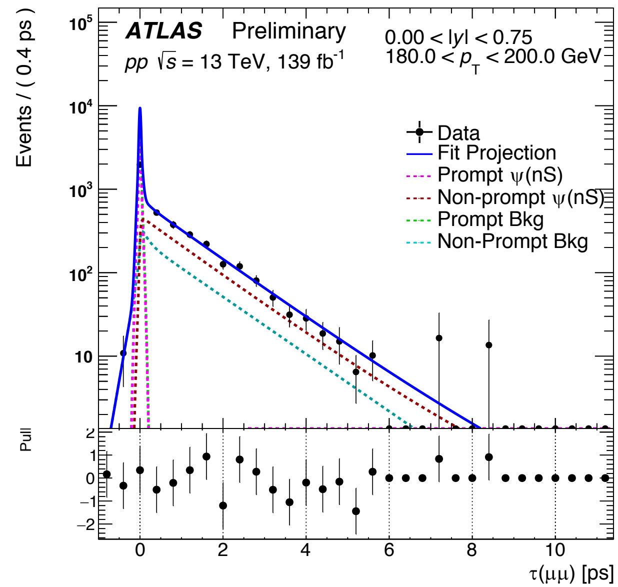

Systematics

Dominated by statistical uncertainty at high p_T

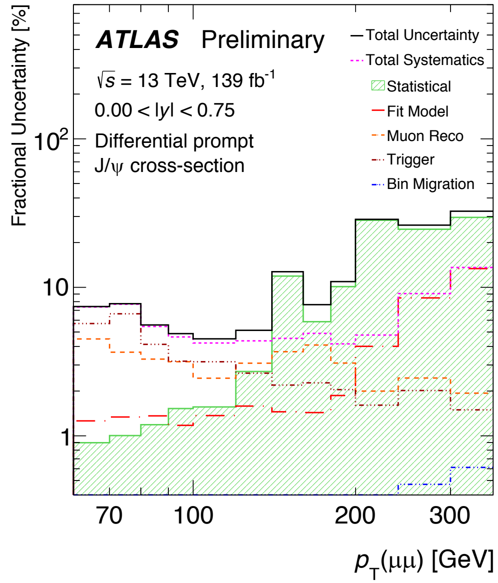

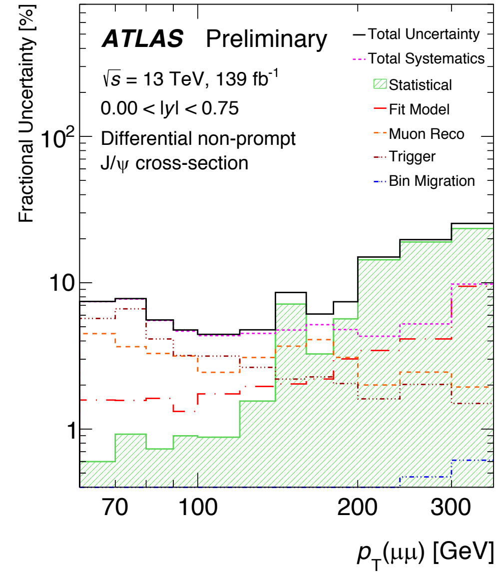

Muon reconstruction and Trigger dominant at low p_T

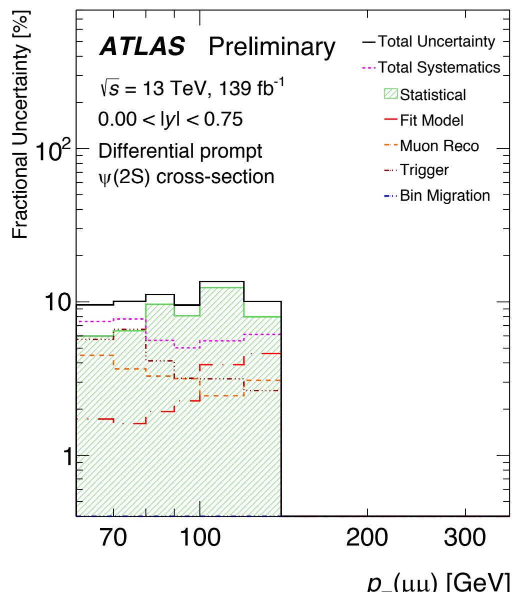

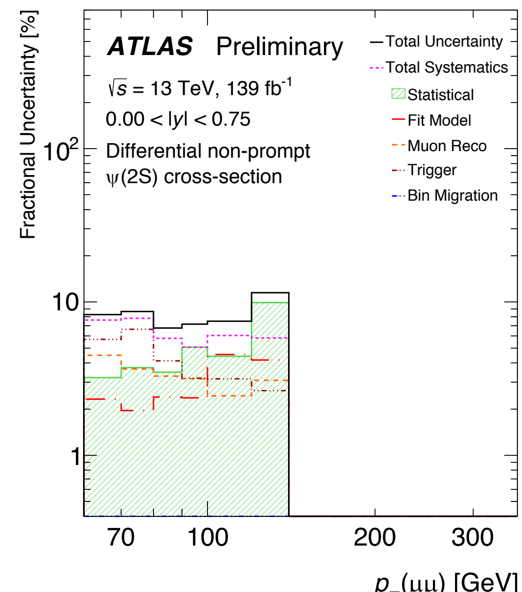

J/ψ prompt and non-prompt

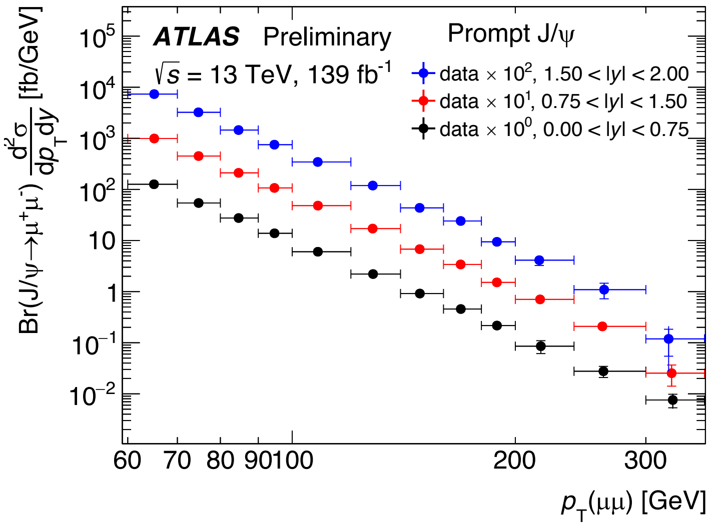

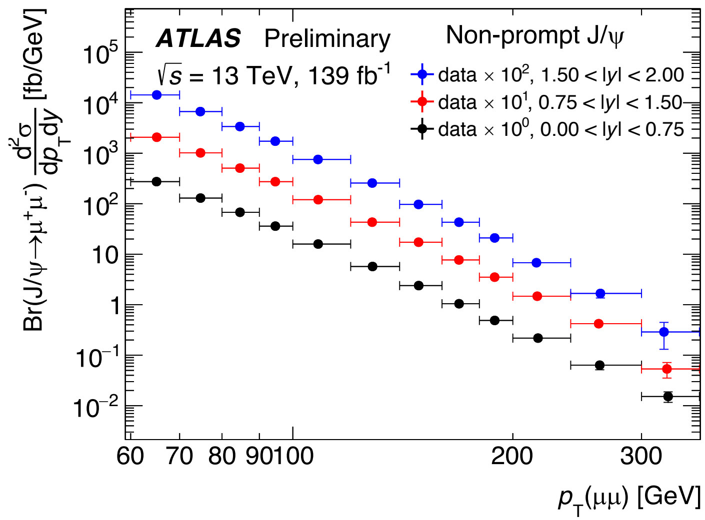

ψ(2S) prompt and non-prompt

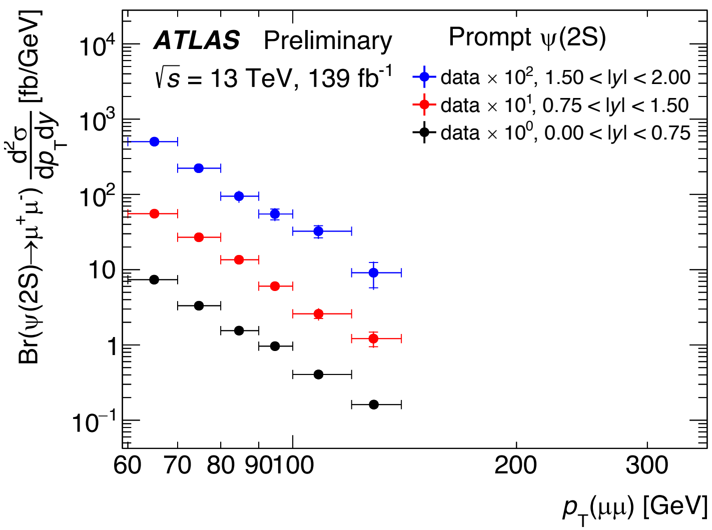

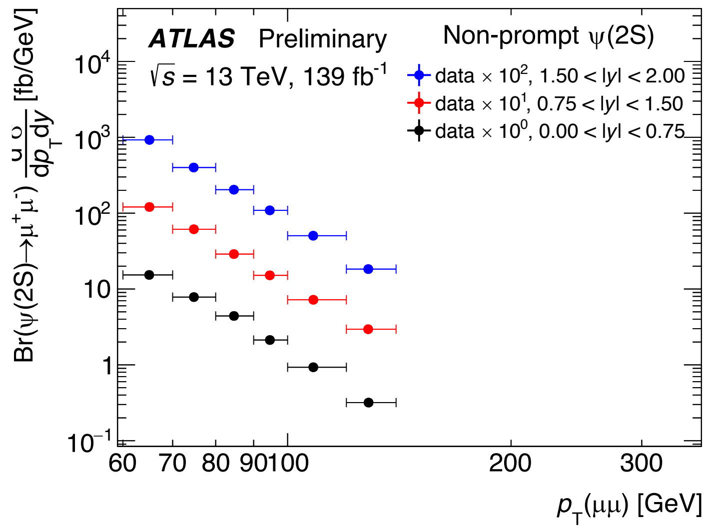

Non-prompt
Production fraction

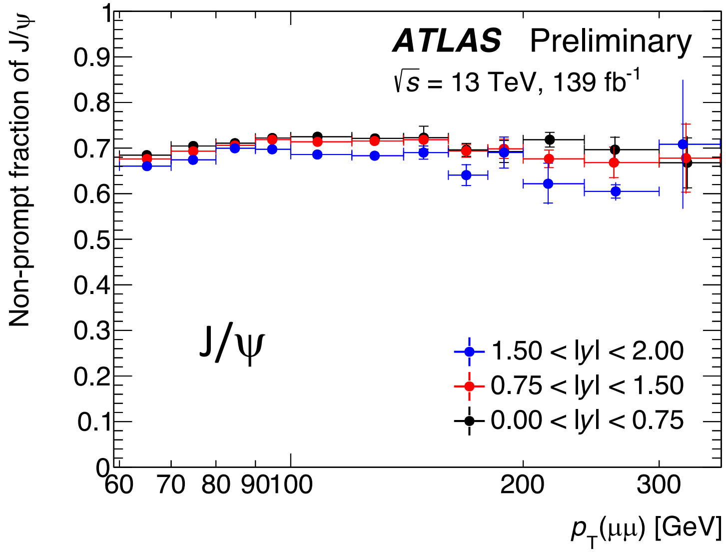

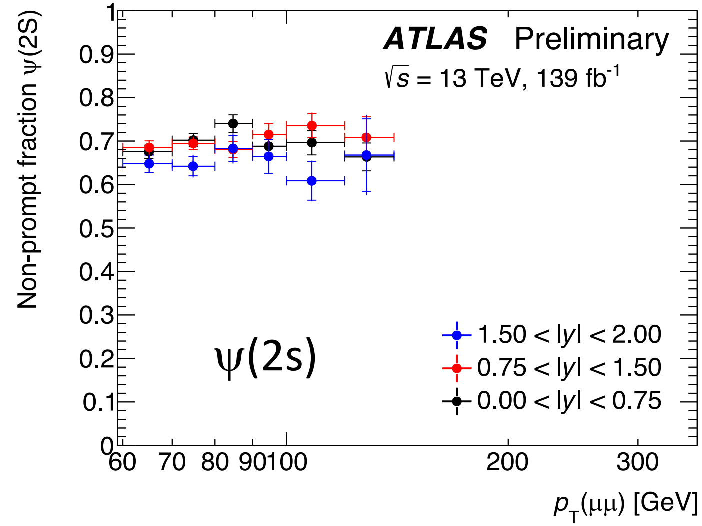

Ratio of ψ(2s) to J/ψ

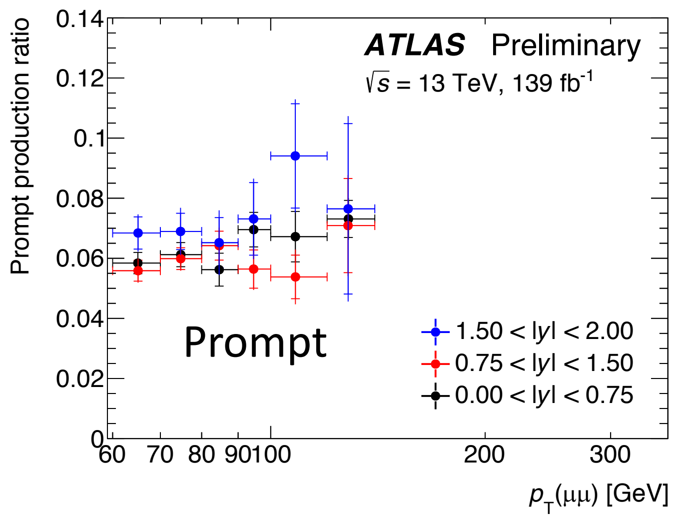

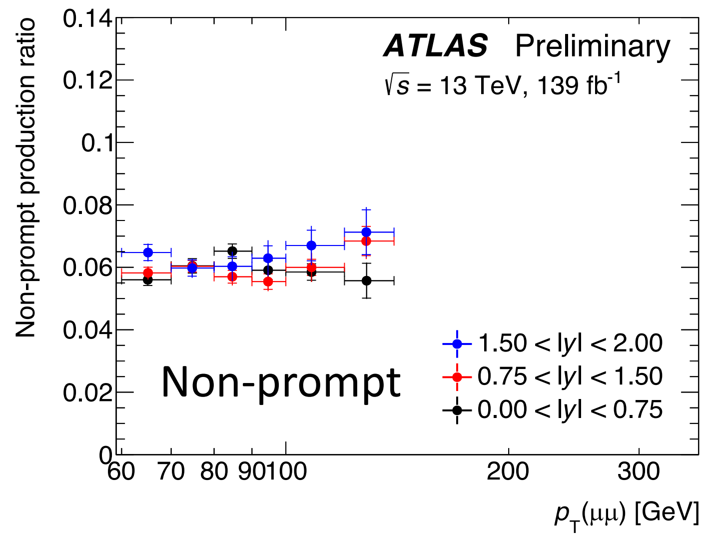

ATLAS and CMS results fit to a simple function

Consistent results with CMS in overlap region

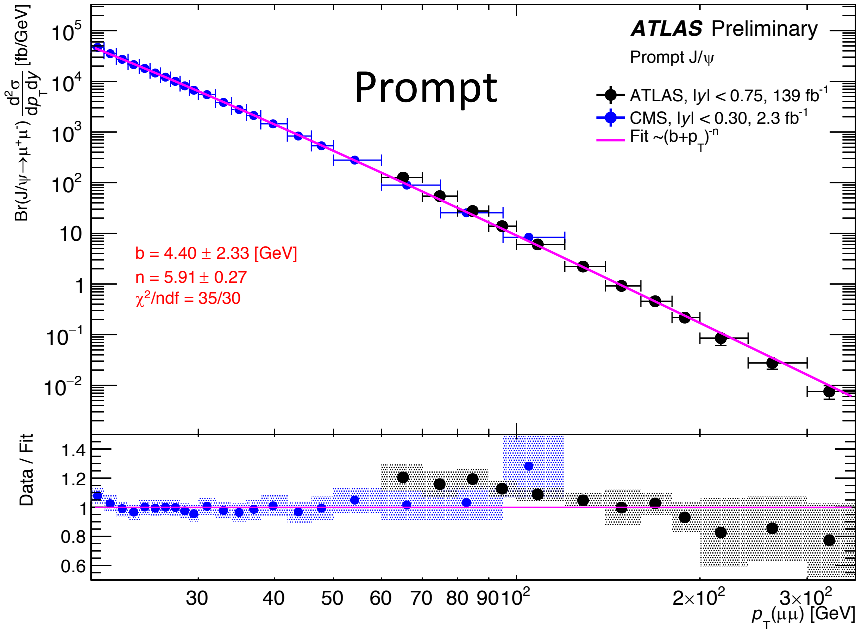

Non Prompt

Comparison to FONLL

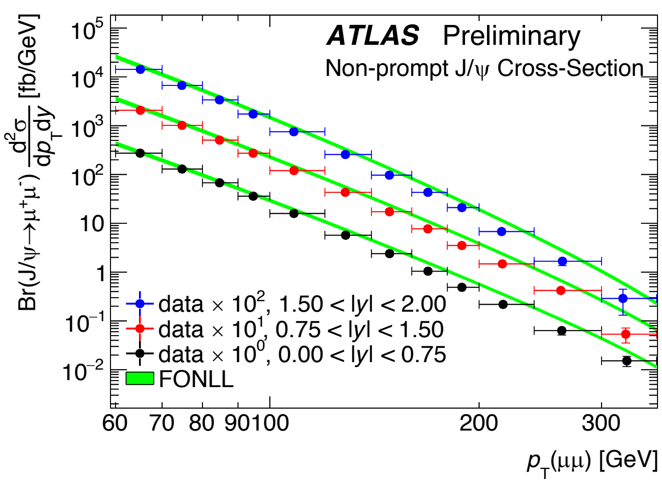

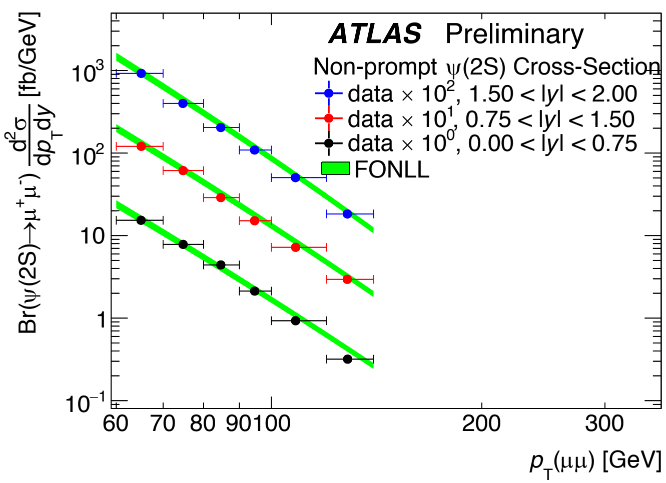

FONLL: JHEP **0103** (2001) 006, JHEP **1210** (2012) 137

Ratio of measurements to FONLL

Good agreement at lower end of p_T range, but FONLL predicting slightly larger cross sections at higher p_T for J/ψ

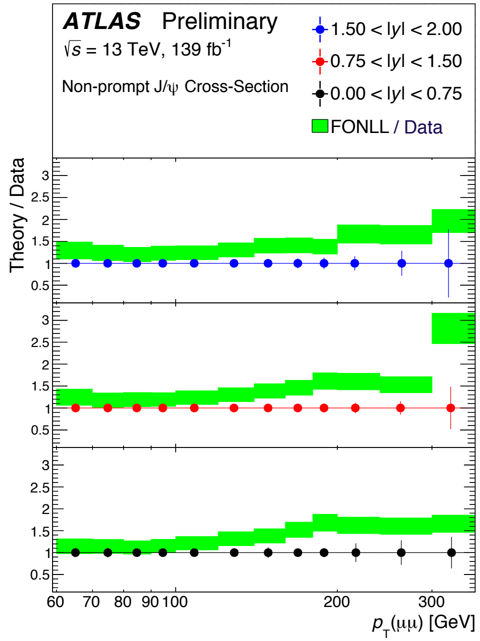

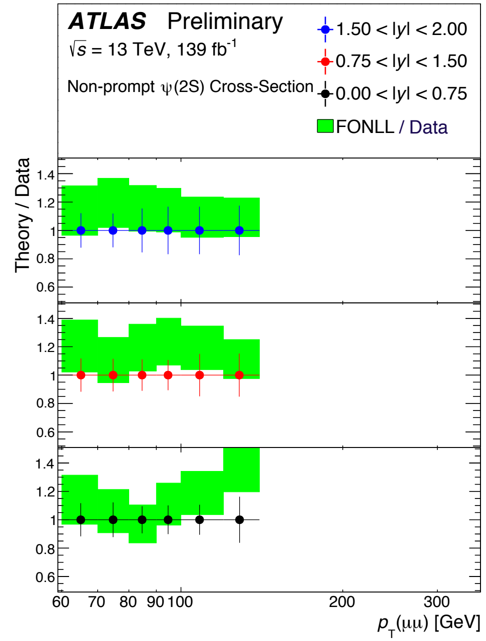

Non-prompt production ratio shows good agreement between data and FONLL

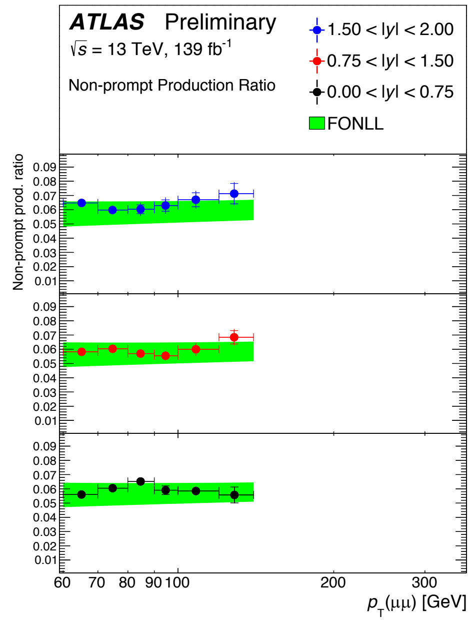

J/ψ production in associated with a W boson at 8 TeV

arXiv: hep-ex 1909.13626

J/ψ production in associated with a W boson at 8 TeV

- Production mechanism of charmonium in hadronic collisions is not fully understood
- Relative contribution of Color Singlet (CS) and Color Octet (CO) is unknown
- Including both CS and CO brings theory and experiment into better agreement
- Requiring an associated object ($W^{\pm}$) filters the possible CS/CO diagrams
- In addition contributions of double parton scattering vs single parton scattering processes unknown. $J/\psi + W^{\pm}$ can probe this using $\Delta\phi$ between the two particles.

Measure $R_{J/\psi}$: Cross section of associated prompt J/ψ +W production divided by cross section of inclusive W production

$$R_{J/\psi} \equiv \frac{\sigma_{W+J/\psi}}{\sigma_W} \equiv \frac{\frac{N_{W+J/\psi}}{\mathcal{T}\times\mathcal{L}\times\epsilon_W\times\mathcal{A}_W\times\epsilon_{J/\psi}\times\mathcal{A}_{J/\psi}}}{\frac{N_W}{\mathcal{T}\times\mathcal{L}\times\epsilon_W\times\mathcal{A}_W}} \equiv \frac{1}{N_W}\left[\frac{N_{W+J/\psi}}{\epsilon_{J/\psi}\times\mathcal{A}_{J/\psi}}\right]$$

Need

N_W: Background subtracted yield for inclusive W

$N_{W+J/\psi}$: Background subtracted yield of prompt W+J/ψ

$\varepsilon_{J/\psi}$, $A_{J/\psi}$: Efficiency and acceptance for J/ψ

Inclusive W sample

$W^{\pm}$ boson selection
At least one isolated muon that originates < 1 mm from primary vertex along z-axis
p_T (trigger muon) > 25 GeV
$\lvert\eta^{\mu}\rvert < 2.4$
Missing transverse momentum > 20 GeV
$m_T(W^{\pm}) > 40$ GeV
$\lvert d_0\rvert/\sigma_{d_0} < 3$

<u>Backgrounds:</u>

W→ eν

W→ τν

Z → ee, μμ, ττ ⟶ N_W

Single t

Diboson

ttbar

Multijet (QCD)

W + J/ψ sample

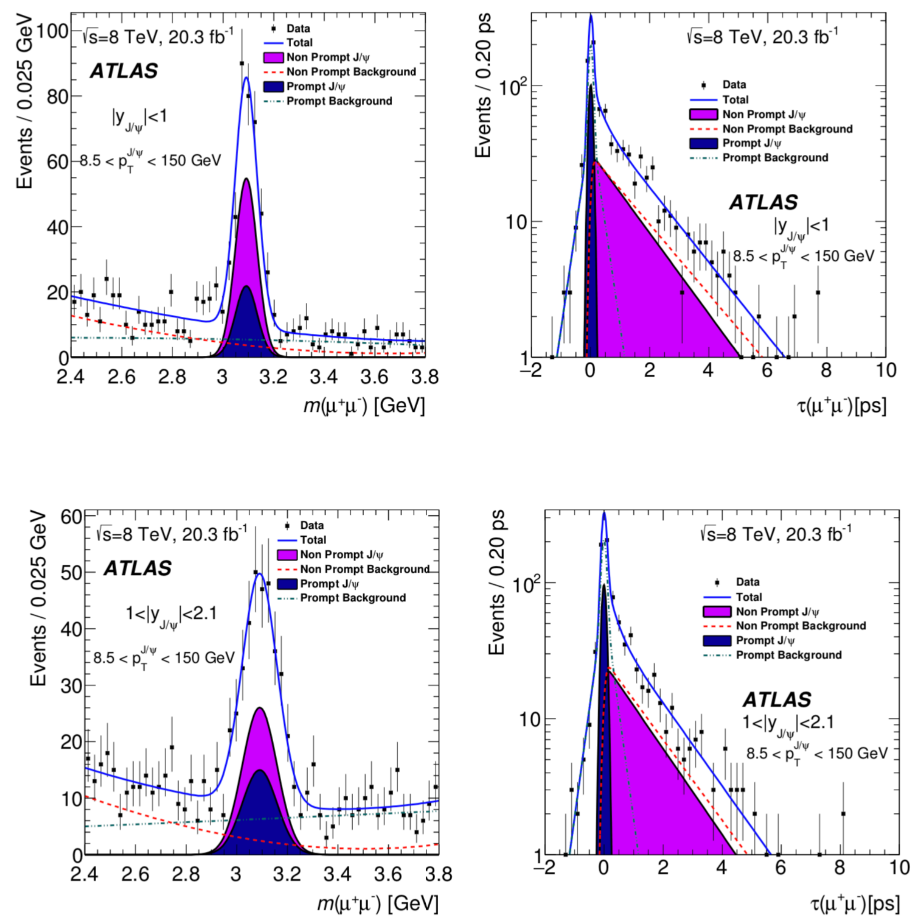

Associated J/ψ + W sample

J/ψ selection
$2.4 < m(\mu^+\mu^-) < 3.8$ GeV
$8.5 < p_T^{J/\psi} < 150$ GeV, $\lvert y_{J/\psi}\rvert < 2.1$
$p_T^{\mu_1} > 4$ GeV, $\lvert \eta^{\mu_1}\rvert < 2.5$
$\left\{ \begin{array}{ll} \text{either } p_T^{\mu_2} > 2.5\text{ GeV}, & 1.3 \le \lvert\eta^{\mu_2}\rvert < 2.5 \\ \text{or } p_T^{\mu_2} > 3.5\text{ GeV}, & \lvert\eta^{\mu_2}\rvert < 1.3 \end{array} \right\}$

Combined mass-lifetime fit to extract prompt J/ψ yield

Backgrounds:
- $B_c \to J/\psi\, l\nu X$
- Multijet (QCD)
- J/ψ+Z
- J/ψ+W ($W \to \tau\nu$)

Pileup:
J/ψ and W produced
in two different collisions

$N_{W+J/\psi}$

$\varepsilon_{J/\psi}$ and $A_{J/\psi}$ determined using p_T and rapidity dependent corrections

Double Parton Scattering

Probability that a J/ψ is produced by a second hard process

$$P^{ij}_{J/\psi|W^{\pm}} = \frac{\sigma^{ij}_{J/\psi}}{\sigma_{\text{eff}}}$$

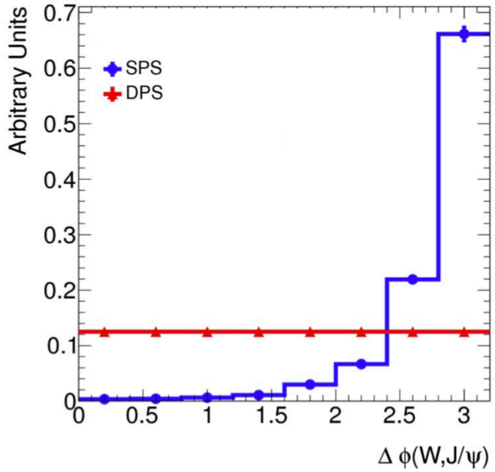

Exact shape of SPS unknown

Effective cross section σ_{eff} is unknown so choose two different values from previous ATLAS measurements

$$\sigma_{\text{eff}} = 15 \pm 3(\text{stat.})^{+5}_{-3}(\text{sys.})\ \text{mb from}\ W^{\pm} + 2\text{-jet events}$$

$$\sigma_{\text{eff}} = 6.3 \pm 1.6(\text{stat.}) \pm 1.0(\text{sys.})\ \text{mb from prompt}\ J/\psi\ \text{pair production}$$

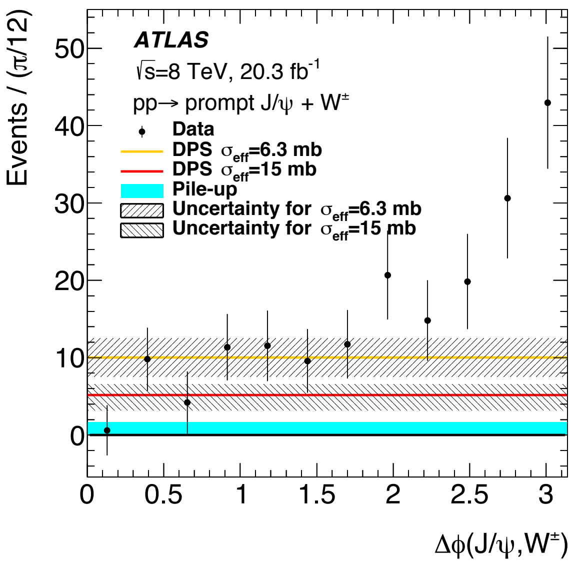

Both values of σ_{eff} consistent with data at low $\Delta\phi$

Systematics:

Source of Uncertainty	Uncertainty [%]	
	$\lvert y_{J/\psi}\rvert < 1$	$1 < \lvert y_{J/\psi}\rvert < 2.1$
J/ψ mass fit	8.7	4.9
Vertex separation	12	15
$\mu_{J/\psi}$ efficiency	2.0	1.6
Pile-up	1.1	1.4
$J/\psi + Z$ and $J/\psi + W^{\pm}(\to \tau^{\pm}\nu)$	3.5	4.8
Efficiency correction	2.3	2.3
J/ψ spin alignment	34	28

Fiducial measurement: Independent of unknown spin-alignment of J/ψ

$$R^{\text{fid}}_{J/\psi} = \frac{\sigma_{\text{fid}}(pp \to J/\psi + W^{\pm})}{\sigma(pp \to W^{\pm})} \cdot \mathcal{B}(J/\psi \to \mu\mu) = \frac{1}{N(W^{\pm})} \sum_{p_{\text{T}} \text{ bins}} [N^{\text{eff}}(J/\psi + W^{\pm}) - N^{\text{fid}}_{\text{pile-up}}],$$

$$R^{\text{fid}}_{J/\psi} = (2.2 \pm 0.3 \pm 0.7) \times 10^{-6}$$

Inclusive measurement: Takes into account unknown J/ψ spin-alignment and J/ψ acceptance

$$R^{\text{incl}}_{J/\psi} = \frac{\sigma_{\text{incl}}(pp \to J/\psi + W^{\pm})}{\sigma(pp \to W^{\pm})} \cdot \mathcal{B}(J/\psi \to \mu\mu) = \frac{1}{N(W^{\pm})} \sum_{p_{\text{T}} \text{ bins}} [N^{\text{eff+acc}}(J/\psi + W^{\pm}) - N_{\text{pile-up}}],$$

$$R^{\text{incl}}_{J/\psi} = (5.3 \pm 0.7 \pm 0.8 \pm 1.7) \times 10^{-6}$$

1st uncertainty: statistical
2nd uncertainty: systematic
3rd uncertainty: spin alignment

Subtract estimated DPS contribution to allow measurement to be compared to theory

$$R^{\mathrm{DPSsub}}_{J/\psi} = (3.6 \pm 0.7^{+1.1}_{-1.0} \pm 1.7) \times 10^{-6}, \quad [\sigma_{\mathrm{eff}} = 15^{+5.8}_{-4.2}\ \mathrm{mb}]$$

$$R^{\mathrm{DPSsub}}_{J/\psi} = (1.3 \pm 0.7 \pm 1.5 \pm 1.7) \times 10^{-6}, \quad [\sigma_{\mathrm{eff}} = 6.3 \pm 1.9\ \mathrm{mb}]$$

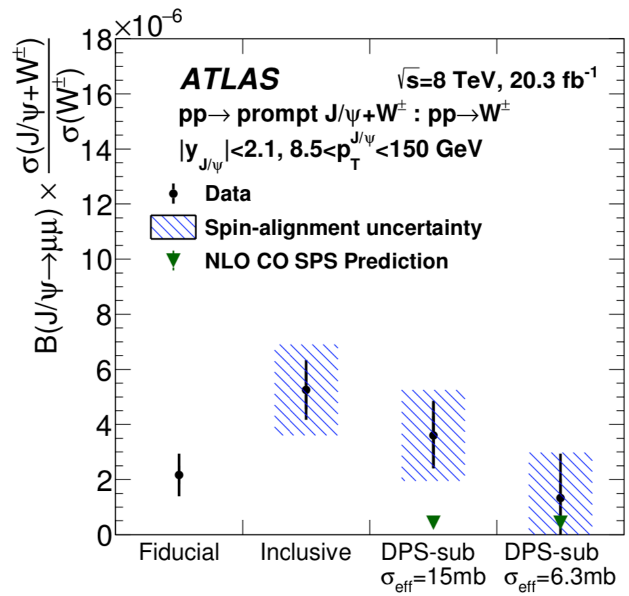

NLO:Phys. Rev. D **53**(1996) 150, 6203

Differential Measurement

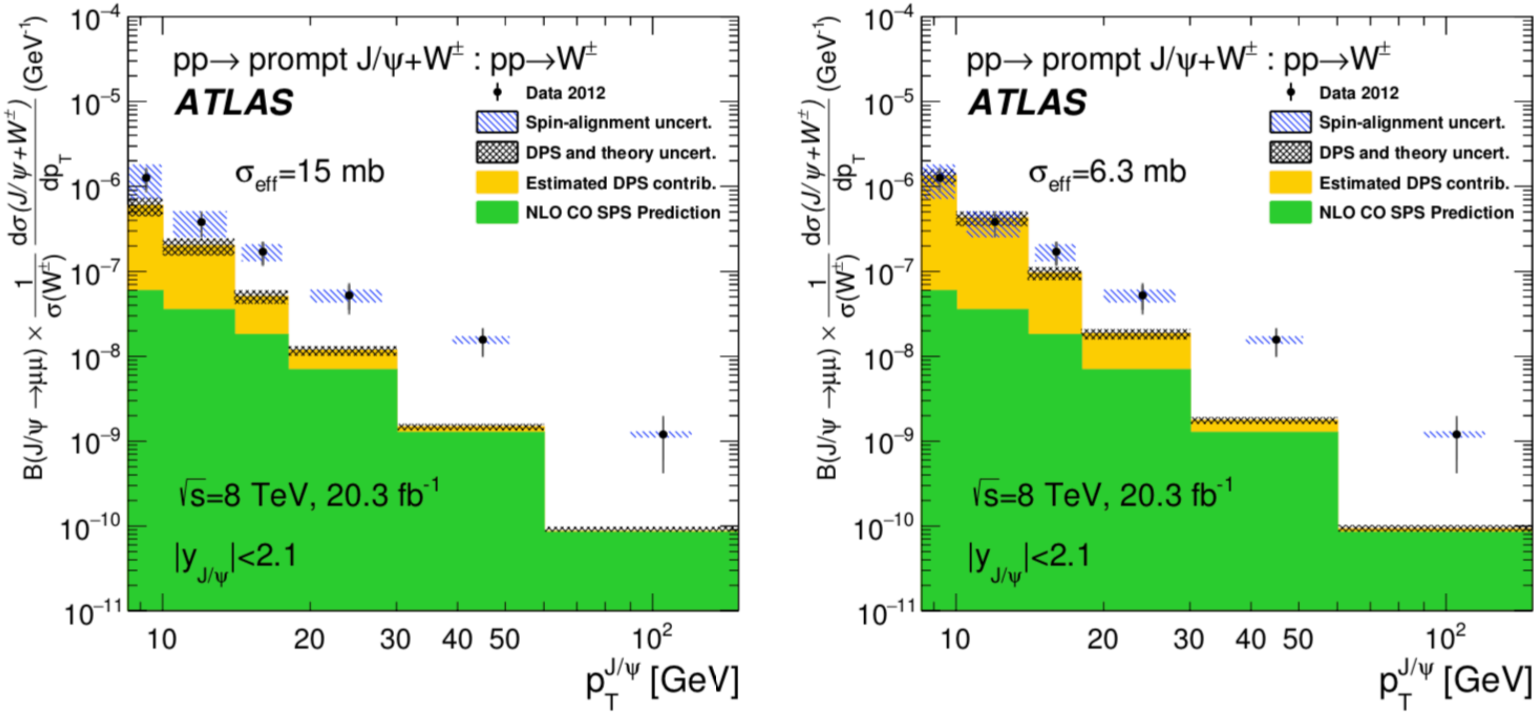

Neither value of σ_{eff} can correctly model J/ψ p_T dependence

Conclusions

Selected measurements in ATLAS heavy flavor production shown

Quarkonia allowing probes of QCD at the perturbative/non-perturbative boundary and in studying effects of Cold Nuclear Matter

For 13 TeV measurement

> Good agreement with previous measurement from CMS

> p_T reach greatly extended

> Non-prompt production of J/ψ consistent with FONLL at low p_T

> FONLL overestimates non-prompt J/ψ cross section at high p_T

Prompt J/ψ + W

> Measurement of $\Delta\phi$ distribution indicates that both SPS and DPS contributions are present in data

> Smaller value of σ_{eff} is preferred

> Neither value of σ_{eff} can describe J/ψ p_T dependence

First measurements with full Run-2 datasets presented, stayed tuned for more interesting results

Additional Material

ATLAS detector and triggers

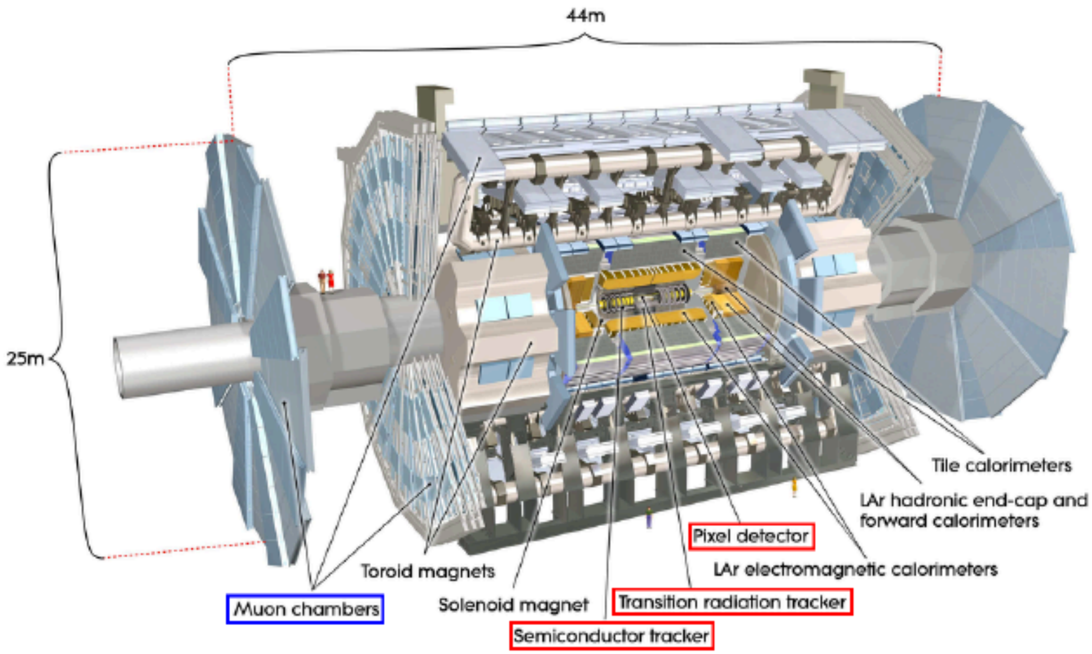

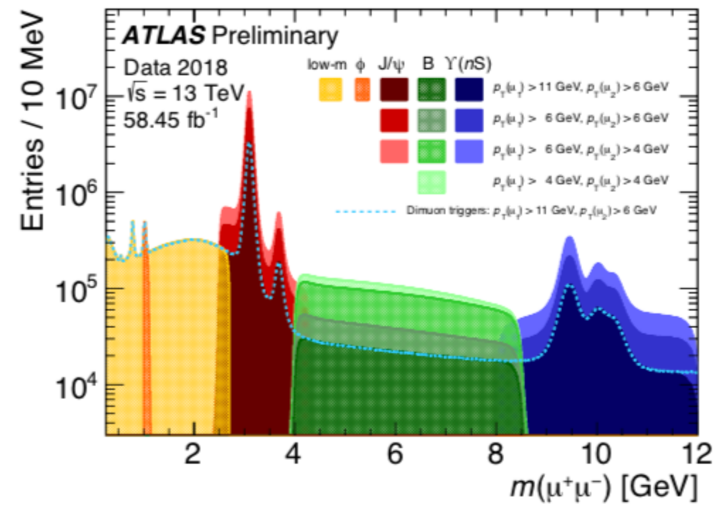

Charmonium Production in Pb-Pb Eur. Phys. J. C78 (2018) 762

i	Type	Source	$f_i(m)$	$h_i(\tau)$
1	J/ψ	p	$\omega\, CB_1(m) + (1-\omega)G_1(m)$	$\delta(\tau)$
2	J/ψ	np	$\omega\, CB_1(m) + (1-\omega)G_1(m)$	$E_1(\tau)$
3	$\psi(2S)$	p	$\omega\, CB_2(m) + (1-\omega)G_2(m)$	$\delta(\tau)$
4	$\psi(2S)$	np	$\omega\, CB_2(m) + (1-\omega)G_2(m)$	$E_2(\tau)$
5	Bkg	p	$E_3(m)$	$\delta(\tau)$
6	Bkg	np	$E_4(m)$	$E_5(\tau)$
7	Bkg	np	$E_6(m)$	$E_7(\lvert\tau\rvert)$

	J/ψ yield		$R_{AA}^{J/\psi}$		$\rho_{PbPb}^{\psi(2S)/J/\psi}$
Source	Uncorr.	Corr.	Uncorr.	Corr.	Uncorr.
Trigger	2 - 4%	3%	5 - 6%	5%	< 1%
Reconstruction	4 - 5%	2%	6 - 7%	2%	< 1%
Fitting	1 - 2%	1%	1 - 2%	1%	8 - 9%
T_{AA}	–	1 - 8%	–	1 - 8%	–
Luminosity	–	–	–	5.4%	–

Quarkonium production in pp and pPb Eur. Phys. J. C 78 (2018) 171

i	Type	Source	$f_i(m_{\mu\mu})$	$h_i(\tau_{\mu\mu})$
1	J/ψ	Prompt	$\omega_1 CB_1(m_{\mu\mu}) + (1-\omega_1)G_1(m_{\mu\mu})$	$\delta(\tau_{\mu\mu})$
2	J/ψ	Non-prompt	$\omega_1 CB_1(m_{\mu\mu}) + (1-\omega_1)G_1(m_{\mu\mu})$	$E_1(\tau_{\mu\mu})$
3	$\psi(2S)$	Prompt	$\omega_2 CB_2(m_{\mu\mu}) + (1-\omega_2)G_2(m_{\mu\mu})$	$\delta(\tau_{\mu\mu})$
4	$\psi(2S)$	Non-prompt	$\omega_2 CB_2(m_{\mu\mu}) + (1-\omega_2)G_2(m_{\mu\mu})$	$E_2(\tau_{\mu\mu})$
5	Background	Prompt	F	$\delta(\tau_{\mu\mu})$
6	Background	Non-prompt	$E_3(m_{\mu\mu})$	$E_4(\tau_{\mu\mu})$
7	Background	Non-prompt	$E_5(m_{\mu\mu})$	$E_6(\lvert\tau_{\mu\mu}\rvert)$

Collision type	Sources	Ground-state yield [%]	Excited-state yield [%]	Ratio [%]
p+Pb collisions	Luminosity	2.7	2.7	–
	Acceptance	1–4	1–4	–
	Muon reco.	1–2	1–2	< 1
	Muon trigger	4–5	4–5	< 1
	Charmonium fit	2–5	4–10	7–15
	Bottomonium fit	2–15	2–15	5–12
pp collisions	Luminosity	5.4	5.4	–
	Acceptance	1–4	1–4	–
	Muon reco.	1–5	1–5	< 1
	Muon trigger	5–7	5–7	< 1
	Charmonium fit	2–7	4–10	7–11
	Bottomonium fit	1–15	2–15	5–12

J/ψ elliptic flow in Pb-Pb Eur. Phys. J. C 78 (2018) 784

i	Type	Source	$f_i(m_{\mu\mu})$	$h_i(\tau_{\mu\mu})$
1	Signal	Prompt	$\omega F_{\mathrm{CB}}(m_{\mu\mu}) + (1-\omega)F_{\mathrm{G}}(m_{\mu\mu})$	$\delta(\tau_{\mu\mu})$
2	Signal	Non-prompt	$\omega F_{\mathrm{CB}}(m_{\mu\mu}) + (1-\omega)F_{\mathrm{G}}(m_{\mu\mu})$	$F_{\mathrm{E}_1}(\tau_{\mu\mu})$
3	Background	Prompt	$F_{\mathrm{E}_2}(m_{\mu\mu})$	$\delta(\tau_{\mu\mu})$
4	Background	Non-prompt	$F_{\mathrm{E}_3}(m_{\mu\mu})$	$F_{\mathrm{E}_4}(\tau_{\mu\mu})$
5	Background	Non-prompt	$F_{\mathrm{E}_5}(m_{\mu\mu})$	$F_{\mathrm{E}_6}(\lvert\tau_{\mu\mu}\rvert)$

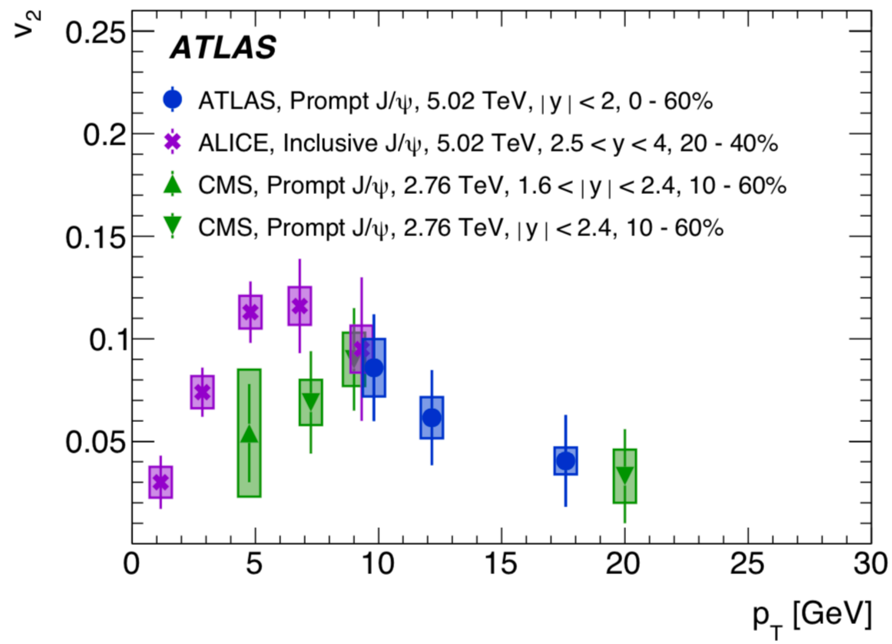

Fit Model

$$\mathrm{PDF}(m,\tau) = \sum_{i=1}^{7} \kappa_i f_i(m) \cdot (h_i(\tau) \otimes R(\tau)) \cdot C_i(m,\tau).$$

i	Type	P/NP	$f_i(m)$	$h_i(\tau)$	$C_i(m,\tau)$
1	J/ψ	P	$\omega G_1(m) + (1-\omega)CB_1(m)$	$\delta(\tau)$	$BV(m,\tau,\rho)$
2	J/ψ	NP	$\omega G_1(m) + (1-\omega)CB_1(m)$	$E_1(\tau)$	1
3	$\psi(2S)$	P	$\omega G_2(m) + (1-\omega)CB_2(m)$	$\delta(\tau)$	1
4	$\psi(2S)$	NP	$\omega G_2(m) + (1-\omega)CB_2(m)$	$E_2(\tau)$	1
5	Bkg	P	B	$\delta(\tau)$	1
6	Bkg	NP	$E_4(m)$	$E_5(\tau)$	1
7	Bkg	NP	$E_6(m)$	$E_7(\|\tau\|)$	1

Notation	Function
G	Gaussian
CB	Crystal Ball
E	Exponential
B	Bernstein polynomials
BV	Correlation term of the bivariate Gaussian dist.

R(τ): Resolution Function

$$\mathrm{BV} \sim \exp\left[\frac{1}{2(1-\rho^2)}\left(\frac{(m-\mu_m)^2}{\sigma_m^2} - \frac{2\rho(m-\mu_m)(\tau-\mu_\tau)}{\sigma_m\sigma_\tau} + \frac{(\tau-\mu_\tau)^2}{\sigma_\tau^2}\right)\right]$$

Reconstruction efficiencies for W+J/ψ and inclusive W samples do not exactly cancel so correction applied

Acceptance depends on the unknown polarization of the J/ψ

$$\frac{d^2N}{d\cos\theta^\star d\phi^\star} \propto 1 + \lambda_\theta \cos\theta^{\star 2} + \lambda_\phi \sin\theta^{\star 2} \cos 2\phi^\star + \lambda_{\theta\phi} \sin 2\theta^\star \cos\phi^\star$$

1. Isotropic (nominal): $\lambda_\theta = \lambda_\phi = \lambda_{\theta\phi} = 0$
2. Longitudinal: $\lambda_\theta = -1$, $\lambda_\phi = \lambda_{\theta\phi} = 0$
3. Transverse-0: $\lambda_\theta = +1$, $\lambda_\phi = \lambda_{\theta\phi} = 0$
4. Transverse-M: $\lambda_\theta = +1$, $\lambda_\phi = -1$, $\lambda_{\theta\phi} = 0$
5. Transverse-P: $\lambda_\theta = \lambda_\phi = +1$, $\lambda_{\theta\phi} = 0$

Largest systematic uncertainty in measurement